

## Solar-heating rates and temperature profiles in Antarctic snow and ice

RICHARD E. BRANDT\* AND STEPHEN G. WARREN

*Geophysics Program AK-50, University of Washington, Seattle, Washington 98195, U.S.A.*

**ABSTRACT.** Observations of temperature maxima at about 10 cm depth in cold Antarctic snow during summer have previously been explained by proposing that solar heating is distributed with depth whereas thermal infrared cooling is localized at the surface (the "solid-state greenhouse"). An increase in temperature from the surface to 10 cm depth ( $\Delta T \approx 4$  K) found by Rusin (1961) on the Antarctic Plateau was successfully reproduced by Schlatter (1972) in a combined radiative-transfer and heat-transfer model. However, when we improve the model's spectral resolution, solving for solar radiative fluxes separately in 118 wavelength bands instead of just one "average" wavelength,  $\Delta T$  shrinks to 0.2 K and moves toward the surface, indicating that the solid-state greenhouse is largely an artifact of inadequate spectral resolution. The agreement between Schlatter's broad-band model and Rusin's measurement suggests that the measurement is inaccurate, perhaps due to solar heating of the buried thermistors. Similar broad-band models which have been applied to the icy surface of Jupiter's satellite Europa are also shown to overestimate the solid-state greenhouse by a factor of about 6.

The reason that the solid-state greenhouse effect is insignificant in the case of Antarctic snow is that the wavelengths which do penetrate deeply into snow (visible light) are essentially not absorbed and are scattered back to the surface, whereas the wavelengths that are absorbed by snow (near-infrared) are absorbed in the top few millimeters.

The conditions needed to obtain a significant solid-state greenhouse are examined. The phenomenon becomes important if the scattering coefficient is small (as in blue ice) or if the thermal conductivity is low (as in low-density snow, such as near-surface depth hoar).

### THE "SOLID-STATE GREENHOUSE"

At the snow surface of an ice sheet, the components of the energy budget are upward and downward solar radiation, upward and downward thermal infrared radiation, turbulent exchange of sensible and latent heat, and conduction of heat through the snow. These energy sources and sinks, along with the radiative and thermal properties of the snow, determine the temperature structure below the snow surface. Temperature gradients in the snow affect ice-grain evolution and therefore the optical properties of the snowpack, and the optical properties in turn affect the vertical distribution of absorbed energy.

The components of the energy budget, as well as the near-surface temperatures in the snow, have often been measured. One of the experiments found a temperature maximum several centimeters below the surface, not just

as a transient but in data averaged over an entire month. This temperature maximum was reported by Rusin (1961) in a study of surface-energy fluxes and temperatures from the IGY station Pioneerskaya, at 2740 m elevation in East Antarctica. Schlatter (1972) succeeded in explaining these temperatures using a model of radiative and conductive energy transfer in snow, which combined to cause a "greenhouse effect", as follows.

Incident solar ("shortwave") radiation (0.3–3  $\mu\text{m}$  wavelength) penetrates to considerable depth in snow, whereas the cooling by emission of thermal infrared ("longwave") radiation to space occurs at the very top surface of the snow. Snow is so opaque in the thermal infrared (3–100  $\mu\text{m}$  wavelength) that radiation emitted by one grain is absorbed by a neighboring grain, so only the topmost grains can lose radiation to space. The shortwave albedo of fine-grained dry snow is 80–85% for Antarctica (Schwerdtfeger, 1970). Since solar radiation penetrates to considerable depth, the 15–20% that is absorbed would cause a heating distributed with depth. Shortwave heating at depth, with longwave cooling at the surface, causes a temperature gradient to support a conductive heat flux upward toward the surface.

The solid-state greenhouse is an attractive idea. It has

\* Present address: 15 Goodrich Street, Canton, New York 13617, U.S.A.

been promoted by many authors, for example in the review article by Warren (1982, section I1).

What we see as a potential flaw in this reasoning is that the absorption coefficient of ice, and therefore of snow, varies with wavelength across the solar spectrum by five orders of magnitude. The 15–20% of the incident solar energy that is absorbed by snow is mostly near-infrared radiation, and we will show that this radiation is absorbed in the topmost few millimeters. For visible light, the albedo of snow is nearly 100%, so the radiation which does penetrate the snow to tens of centimeters (and for example brightens a snow cave) is scattered repeatedly by snow grains and eventually re-emerges at the surface.

On the other hand, it is indeed adequate to treat the thermal infrared emission by snow without taking account of spectral variation, because at all wavelengths in the thermal infrared spectrum the mean distance that a photon travels in snow before being absorbed is less than one-half mm. Thus, infrared cooling to the sky does occur just at the top surface. Therefore, in this paper, we investigate the effect on Schlatter's model of improving just one term in the surface-energy budget: the solar radiation.

Several models of the greenhouse effect in snow have appeared recently, using the broad-band approximation and obtaining elevated sub-surface temperatures. Colbeck (1989) used such a model to study radiationally induced snow-crystal metamorphism. His analytic model was meant to be illustrative rather than quantitative, as it has a number of simplifying assumptions. For the example of snow on a polar ice sheet (his fig. 10), Colbeck's annual average temperature profile is similar to Schlatter's December temperature profile in predicting  $\Delta T \sim 5$  K for the condition modeled by Schlatter (solar flux  $400 \text{ W m}^{-2}$  and surface albedo 0.84), although the peak is at 20 cm below the snow surface rather than 10 cm. This difference is primarily due to Colbeck's use of a low ( $0.21 \text{ W m}^{-1} \text{ K}^{-1}$ ) conductivity, half that used by Schlatter. Colbeck used the resulting temperatures to calculate crystal-growth rates caused by "radiation recrystallization", and found a sub-surface growth-rate peak at 25 cm (his fig. 12). But he showed that diurnal surface-temperature oscillations imposed in the model, without any solar radiation penetration, will also cause snow-crystal growth, although at lower rates and without a sub-surface peak. Colbeck found that, for seasonal snow, the observed growth rates are smaller than those calculated by the model. He attributed this discrepancy to a lack of sunny conditions on average seasonal snow, but we will show that it could instead be caused by the broad-band assumption in the treatment of solar radiation.

Brown and Matson (1987) and Matson and Brown (1989) used a model similar to Schlatter's and calculated large sub-surface temperature maxima for snow-like surfaces on satellites of the outer planets, in particular Jupiter's satellite Europa. They argued that a broad-band approximation for solar radiation was adequate because contamination of the snow (inferred from the observed albedo of about 60%) makes the medium "grey" across the solar spectrum. Although this would be true for snow grossly contaminated with enough carbon to bring the albedo down much lower, we show below

that the broad-band approximation is inadequate for the moderately contaminated snow of 60% albedo modeled by Matson and Brown.

## TEMPERATURE MEASUREMENTS

Not all measurements of snow temperature show the sub-surface maximum. At Pioneerskaya in December, Rusin measured the temperature at 10 cm depth to be 3.7 K higher than at the snow surface. However, more recent studies at the South Pole by Carroll (1982) and in the Arctic by Ohmura (1984) did not find sub-surface maxima. Ohmura concluded that the bulk of absorbed radiation must occur at the surface to account for the lack of melting under the radiative conditions he measured. Furthermore, laboratory experiments by Ishikawa and Ishida (1970) suggest that vertical inhomogeneity of the snow is a necessary condition for a sub-surface temperature maximum.

This evidence is in disagreement with the sub-surface temperature maximum modeled by Schlatter and observed by Rusin. An explanation for Rusin's measurements could be radiative heating of sub-surface thermistors, so that they were not recording the true snow temperature. As we show below, variations in boundary conditions, such as vertical variation of grain-size and density or an underestimation of the sensible- and latent-heat flux are not likely to be capable of causing such a large temperature maximum at 10 cm depth. We are also confident that the snow at Pioneerskaya was not significantly contaminated, because its measured albedo was over 80%.

We show below that the solar heating is concentrated in the top few millimeters of the snow surface. In most measurements of snow temperature (including ours, presented below), the vertical resolution was too coarse to discover a possible temperature maximum *within* the top centimeter. However, Alley and others (1990) have very recently done this in Greenland; their results are discussed below.

## EXTINCTION COEFFICIENT FOR SOLAR RADIATION

Radiation intensity at a particular wavelength  $\lambda$  is attenuated exponentially in a medium which only absorbs light and does not scatter it. Radiative flux  $F$  is in general not attenuated exponentially with depth  $z$ . However, at sufficient optical depth below the surface, in a uniform medium which both absorbs and scatters light, the downward flux  $F \downarrow$  is indeed attenuated approximately exponentially (a few millimeters depth in snow is usually sufficient to reach the exponential regime):

$$F \downarrow (z + \Delta z, \lambda) = F \downarrow (z, \lambda) \exp(-k_\lambda \Delta z) \quad (1)$$

where  $k_\lambda$  is the "asymptotic flux-extinction coefficient" at wavelength  $\lambda$  (Warren, 1982, section I). Plots of  $\ln|F \downarrow (z, \lambda)/F \downarrow (0, \lambda)|$  versus  $z$  based on observations with narrow band-pass filters in homogeneous snow or ice of uniform density are approximately straight lines with

slope =  $-k_\lambda$ . Such plots have been presented by Liljequist (1956, fig. 51) and Grenfell and Maykut (1977, fig. 4).

Straight lines will not be obtained if the filter's band pass is too large, because  $k$  varies with  $\lambda$ . In particular, extinction of the total solar energy in snow has often been measured, using pyranometers (Coulson, 1975, chapter 4) that collect all radiation energy from 0.2 to 2.8  $\mu\text{m}$  wavelength. An illustrative result is figure 1 of Schwerdtfeger and Weller (1977); reproduced by Warren (1982) for a filter with a band pass from 0.3 to 0.7  $\mu\text{m}$ , showing not a straight line but instead  $k$  decreasing from the surface to 1 m depth in Antarctic snow. This is because the wavelengths with large  $k$  are attenuated rapidly and are essentially filtered out by the top layers of snow, so that at greater depth the remaining solar energy consists predominantly of wavelengths with smaller  $k$ .

The figure of Schwerdtfeger and Weller indicates that it would be futile to search for a single value of flux-extinction coefficient that could be used at all depths for clean snow. Yet, many investigators have attempted to measure just that, and their results were reviewed by Mellor (1977), who, not surprisingly, found great disagreement among them. They are required, however, by models that treat the solar radiation as a single broad band, such as those of Schlatter, Matson and Brown, and Colbeck. At great depth in the snow, the overlying snow is itself an effective filter, leaving only the radiation near  $\lambda = 0.47 \mu\text{m}$  (where  $k$  is minimum) to continue penetrating downward in the snow. Therefore, measurements at depth, even with non-selective pyranometers, can obtain consistent straight-line fits to the plot of  $\log F_\lambda \downarrow$  vs  $z$ . Because of their consistency, it is these measurements that were favored for broad-band modeling, so they exaggerated the depth at which radiation is absorbed.

In summary, the extinction coefficient for the total solar energy, sometimes called the "bulk-extinction

coefficient", decreases with increasing depth in the snow because the spectral composition of the downward flux changes. However, it is important to distinguish whether this bulk-extinction coefficient is defined so as to be used for computing heating rates or instead for explaining measurements of downward flux. In order to compute heating rates, Grenfell and Maykut (1977) defined what we will call the *net* bulk-extinction coefficient  $k_{\text{GM}}(z)$  as a weighted average of  $k_\lambda$  over  $\lambda$ , weighted by the *net* flux at each wavelength:

$$k_{\text{GM}}(z) = \frac{\int [k_\lambda(1 - a_\lambda)F_\lambda \downarrow(0) \exp(-k_\lambda z)] d\lambda}{\int [(1 - a_\lambda)F_\lambda \downarrow(0) \exp(-k_\lambda z)] d\lambda} \quad (2)$$

where  $k_\lambda$ ,  $a_\lambda$ ,  $F_\lambda \downarrow(0)$  are the spectral flux-extinction coefficient, spectral albedo and spectral solar flux, respectively. Grenfell and Maykut found  $k_{\text{GM}}$  to decrease by a factor of 50 from the surface to 12 cm depth in multi-year white sea ice. Choudhury (1981) calculated  $k_{\text{GM}}$  to decrease by a factor of 150 in the top 12 cm of fine-grained dry snow.

For comparison with measured downward radiation fluxes such as those of Schwerdtfeger and Weller, a "downward bulk extinction coefficient" is appropriate, which describes the local (i.e. at level  $z$ ) attenuation rate of the *downward* flux:

$$\bar{k}(z) = - (1/\Delta z) \ln \left[ \frac{\int F_\lambda \downarrow(0) \exp[-k_\lambda(z + dz)] d\lambda}{\int F_\lambda \downarrow(0) \exp(-k_\lambda z) d\lambda} \right]. \quad (3)$$

The denominator is the spectrally integrated downward flux at depth  $z$  and the numerator is the spectrally integrated downward flux at depth  $z + \Delta z$ . In this paper, we compute and discuss  $\bar{k}$ , not  $k_{\text{GM}}$ .

Table 1. Standard values of input variables used in the models. (In Figures 9 and 10 some of these are varied away from their standard values.)

	Antarctic snow	Antarctic blue ice	Europa
Incident solar flux ( $\text{W m}^{-2}$ )	400	400	17.4
Downward longwave flux ( $\text{W m}^{-2}$ )	178	178	0
Net downward sensible- plus latent-heat flux at surface ( $\text{W m}^{-2}$ )	-17.6	-17.6	0
Snow-grain radius ( $\mu\text{m}$ )	100	-	100
Carbon soot (ppm by mass)	0	0	10
Thermal conductivity ( $\text{W m}^{-1} \text{K}^{-1}$ )	0.5	2.1	0.01
Longwave emissivity	0.98	0.98	0.98
Density ( $\text{kg m}^{-3}$ )	380	917	150
Spectrally integrated albedo	0.81 (clear sky) 0.88 (under cloud)	0.07	0.60
Depth interval $\Delta z$ (for computation)	2.5 cm (0.1 mm; Fig. 5)	2.5 cm	2.5 cm
Time interval $\Delta t$ (for computation)	90 s	90 s	1000 s

**MODEL OF RADIATIVE TRANSFER AND HEAT TRANSFER**

To investigate the importance of accounting for spectral detail in shortwave absorption, we use Schlatter’s model, which treats radiative transfer by the popular two-stream approximation. Bohren (1987) has shown that the two-stream model adequately explains the measured spectral albedo of snow. We use the same boundary conditions that Schlatter used, as given either by him or by Rusin for December conditions at Pioneerskaya. These include snow density, average solar flux, average downward longwave radiation, net sensible- and latent-heat exchange at the surface, thermal conductivity of snow and surface albedo, as given in Table 1.

For the spectral version of the model, we need in addition the incident solar spectrum  $F_{\lambda} \downarrow(0)$  and the spectral extinction coefficients  $k_{\lambda}$  calculated from an appropriate radiative-transfer model for dry snow, to determine a downward bulk extinction coefficient  $\bar{k}(z)$ .

The incident solar spectrum at the surface was obtained using the atmospheric radiation model “ATRAD” described by Wiscombe and others (1984), with the incident solar spectrum at the top of the atmosphere given by Labs and Neckel (1970), and Neckel and Labs (1984). We made use of solar spectra which had been calculated for the Antarctic Plateau by Wiscombe and Warren (1980b). These used the ATRAD model applied to summertime atmospheric conditions at Plateau Station, both for clear-sky and for overcast cloud. Since we want to bracket the possible variations in the solar spectrum, for the cloudy sky we use the thickest cloud (i.e. least transmittance) found by Kuhn and others

(1977) at Plateau Station, Antarctica. These solar spectra are shown in Figure 1.

These calculated solar fluxes had to be scaled to be consistent with the input data used by Schlatter. Each spectrum in Figure 1 was scaled so that its integral matched the value reported by Rusin ( $400 \text{ W m}^{-2}$ ). The spectrally averaged albedo measured at Pioneerskaya ( $\alpha = 0.84$ ) corresponds to our calculation for grain radius  $r = 100 \mu\text{m}$  for an average of clear and cloudy sky; our calculated albedo under clear sky is  $\alpha = 0.843, 0.813, 0.779$  for  $r = 50, 100, 200 \mu\text{m}$ , respectively, and about 0.07 higher under cloudy sky. Antarctic surface-snow grains are usually  $50\text{--}200 \mu\text{m}$  in radius. For many of our calculations, we use a standard grain radius of  $100 \mu\text{m}$ . (We use the symbol  $a_{\lambda}$  for spectral albedo;  $\alpha$  for spectrally averaged albedo.)

The remaining figures compare the spectral model to the broad-band model. We first examine the linear absorption coefficient  $\sigma_a$  (units of inverse length), which is the reciprocal of the mean distance a photon travels in snow before being absorbed. The spectrally integrated value  $\bar{\sigma}_a$ , in Schlatter’s two-stream model is obtained as

$$\bar{\sigma}_a = \bar{k}(1 - \alpha)/(1 + \alpha). \tag{4}$$

For the spectral version of the model  $\sigma_a(\lambda)$  is obtained as

$$\sigma_a = \sigma_e - \sigma_s = \sigma_e(1 - \bar{\omega}) \tag{5}$$

where  $\bar{\omega}$  is the single-scattering albedo ( $\bar{\omega} = \sigma_s/\sigma_e$ ). The single-scattering albedo is the probability that a photon survives an encounter with a snow grain by scattering rather than being absorbed. It is to be distinguished from the albedo  $a_{\lambda}$  measured at the snow surface, which is a multiple-scattering albedo, such that  $a_{\lambda} \approx \bar{\omega}^n$ , where  $n$  is the average number of scattering events undergone by a photon before it eventually re-emerges from the snow surface and is counted as part of the albedo. For example, at  $\lambda = 0.5 \mu\text{m}$  in the visible,  $\bar{\omega} \approx 0.999995$  (figure 3 of Wiscombe and Warren (1980a)) for a snow grain of radius  $100 \mu\text{m}$ , and  $n \approx 4000$ , giving  $a_{\lambda} \approx 0.98$  (figure 8 of Wiscombe and Warren (1980a)).

Equation (5) just says that the extinction coefficient  $\sigma_e$  is the sum of the scattering coefficient  $\sigma_s$  and the absorption coefficient  $\sigma_a$  (all are functions of wavelength). The extinction coefficient  $\sigma_e$  is the extinction cross-section area per unit volume (units  $\text{m}^2 \text{m}^{-3}$ ):

$$\sigma_e = N\pi r^2 Q_{\text{ext}}$$

where  $\pi r^2$  is the geometric cross-sectional area of a snow grain of radius  $r$ ,  $Q_{\text{ext}}$  is the “extinction efficiency”, the ratio of extinction cross-section to geometric cross-section, and  $N$  is the number of snow grains per unit volume:

$$N = 3\rho_{\text{snow}}/4\pi r^3 \rho_{\text{ice}}$$

where  $\rho_{\text{snow}}$  is the density of the snowpack and  $\rho_{\text{ice}}$  is the density of pure ice. So, expressing  $\sigma_a$  in terms of the quantities plotted by Wiscombe and Warren (1980a),

$$\sigma_a(\lambda) = Q_{\text{ext}}(\lambda)[1 - \bar{\omega}(\lambda)] \frac{3\rho_{\text{snow}}}{4r\rho_{\text{ice}}}. \tag{6}$$

The spectral absorption coefficient  $\sigma_a(\lambda)$  is plotted in

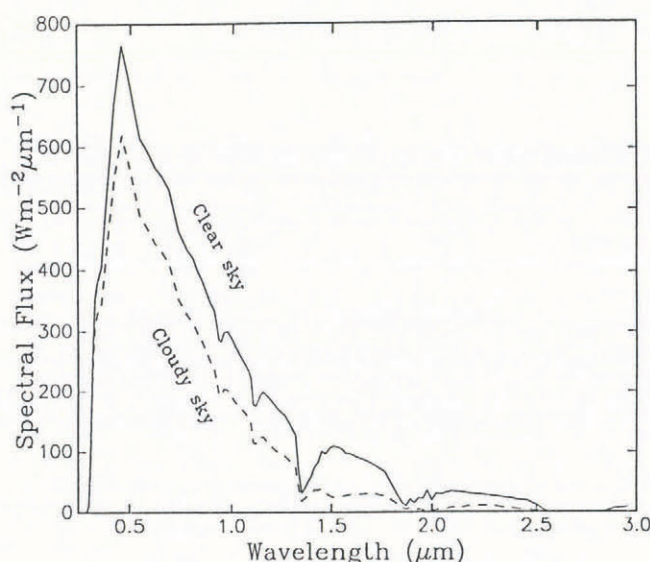


Fig. 1. Downward solar spectrum at the surface of the Antarctic Plateau (surface pressure 680 mbar) calculated for a solar zenith angle of  $66^\circ$  using the model of Wiscombe and others (1984), for clear sky and for the optically thickest cloud condition encountered by Kuhn and others (1977) at Plateau Station. For use in the model of heat transfer in snow, these spectra were scaled so that their integrals matched the value reported by Rusin (1961) and used by Schlatter (1972),  $400 \text{ W m}^{-2}$ .

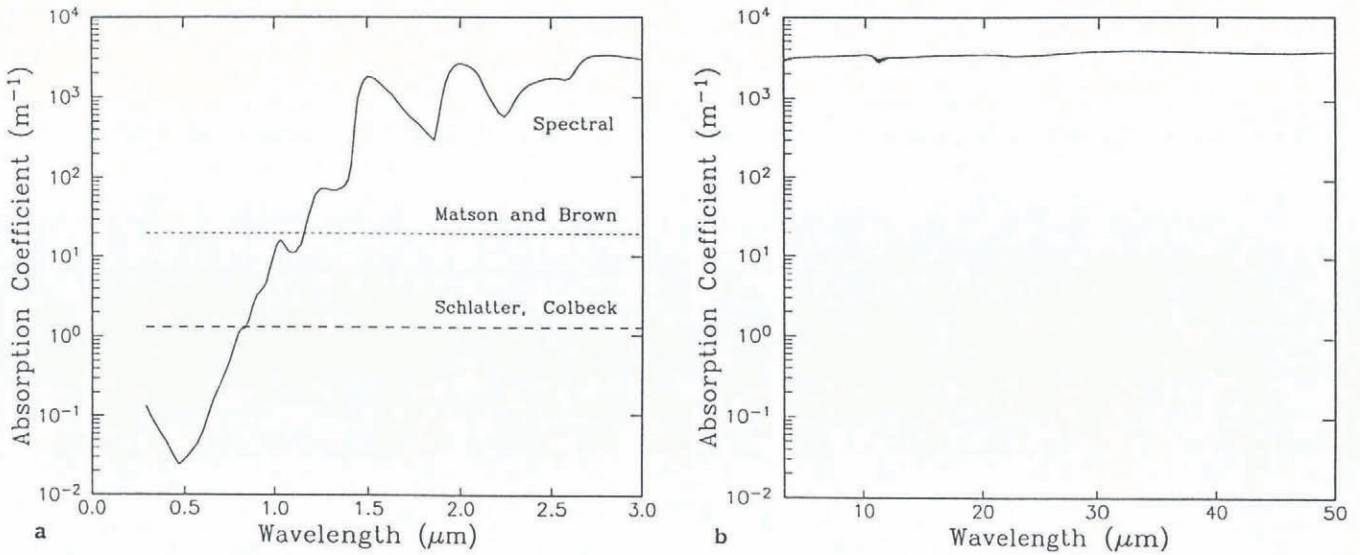


Fig. 2. Absorption coefficient of snow as a function of wavelength, for snow-grain radius  $100 \mu\text{m}$  and density  $400 \text{ kg m}^{-3}$ , calculated using Mie theory (method of Wiscombe (1980)) applied to optical constants measured by Grenfell and Perovich (1981) and reviewed by Warren (1984). Values used by Schlatter (1972), by Colbeck (1989) and by Matson and Brown (1989) are also shown. Matson and Brown's value is higher because they assumed dirty snow of albedo 0.6.

Figure 2a, and compared with the “average” values used in the published broad-band models. The minimum value of  $\sigma_a$  is at  $\lambda = 0.47 \mu\text{m}$  (blue); this wavelength penetrates farthest into snow and is also least absorbed by snow. Although the use of a broad-band value of  $\sigma_a$  seems inappropriate for the solar spectrum, the small variation and large values of  $\sigma_a$  in the thermal infrared between 3 and  $50 \mu\text{m}$ , plotted in Figure 2b, support the assumption that across the thermal infrared spectrum cooling occurs virtually at the surface.

Spectral flux-extinction coefficients in the snow were obtained using the model of Wiscombe and Warren (1980a). The formula for this extinction coefficient (not given in that paper) is as follows:

$$k_\lambda = \sigma_e \{ (1 - \bar{\omega})(1 - \bar{\omega}g) \}^{\frac{1}{2}} \quad (7)$$

where  $g$  is the “asymmetry factor”, the average value of the cosine of the scattering angle. In Schlatter's two-stream model, photons move only in the vertical direction, so that the average cosine for back-scattering is  $\bar{\mu}^- = -1$ , and for forward-scattering is  $\bar{\mu}^+ = +1$ . The asymmetry factor  $g$  is a weighted average of  $\bar{\mu}^+$  and  $\bar{\mu}^-$ :

$$g = b\bar{\mu}^- + (1 - b)\bar{\mu}^+$$

where  $b$  is the back-scattered fraction.

A downward bulk-extinction profile in the top 10 cm of the snowpack (for snow-grain radius  $100 \mu\text{m}$  under clear sky) is shown in Figure 3 compared with the values used by Matson and Brown, Schlatter and Colbeck. It is clear from Figure 3 that measurements of broad-band extinction taken well below the surface are not valid close to the surface. Furthermore, measurements made in the visible spectrum neglect the near-infrared part of the solar spectrum which is responsible for the high near-surface extinction values.

Next, we put the  $\bar{k}$  from Figure 3 into Schlatter's two-stream radiative-transfer model and compute the

absorbed radiant energy as a function of depth. While both the broad-band and spectral models have nearly the same albedo, and hence the same total absorbed energy, Figure 4 shows that the absorbed energy is distributed with depth quite differently in the two models. While the broad-band model shows significant heating continuing to 100 mm depth and below, the spectral model shows that over half of the energy is actually deposited in the top 2 mm. Figure 5 is an expanded view of the uppermost part of Figure 4, for combinations of three grain-sizes and

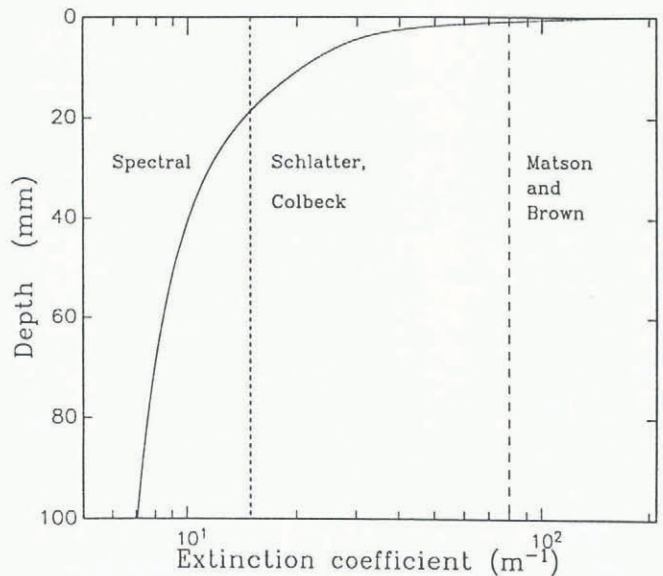


Fig. 3. Downward bulk-extinction coefficient (Equation (3)) as a function of depth in the top 10 cm of the snow, using spectral absorption coefficient from Figure 2 and clear-sky incident solar spectrum from Figure 1. Matson and Brown used a larger extinction coefficient than Schlatter because they assumed dirty snow of albedo 0.6.

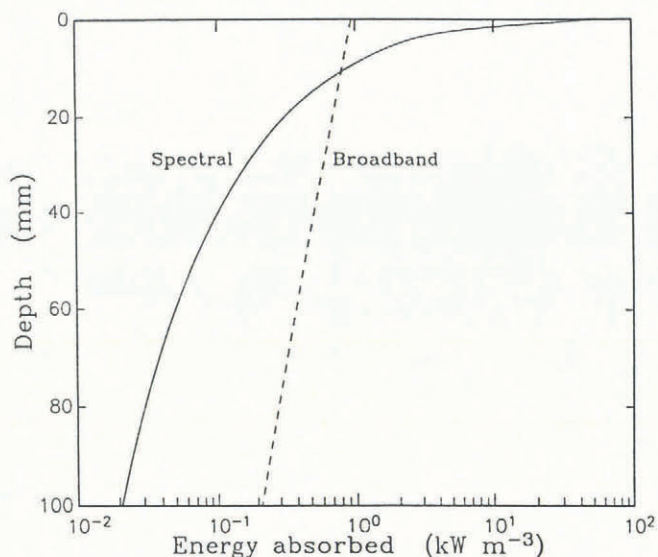


Fig. 4. Solar energy absorbed per unit volume (heating rate) as a function of depth in the top 10 cm of the snow, comparing Schlatter's broad-band model with the spectral model. The incident solar flux is  $400 \text{ W m}^{-2}$ , appropriate for the Antarctic Plateau in December.

the two solar spectra from Figure 1. For snow of  $100 \mu\text{m}$  grain radius under a clear sky, 44% of the total energy is absorbed in the top millimeter. Most of this absorbed energy is in the red and near-infrared part of the spectrum. While the blue light does penetrate deep into the snow, almost all of it is eventually scattered back to the surface, where it exits and does not contribute to radiative heating. (Less energy is absorbed near the surface under the cloudy sky, because the cloud absorbs some of the near-infrared radiation which otherwise would have been absorbed by the surface snow.)

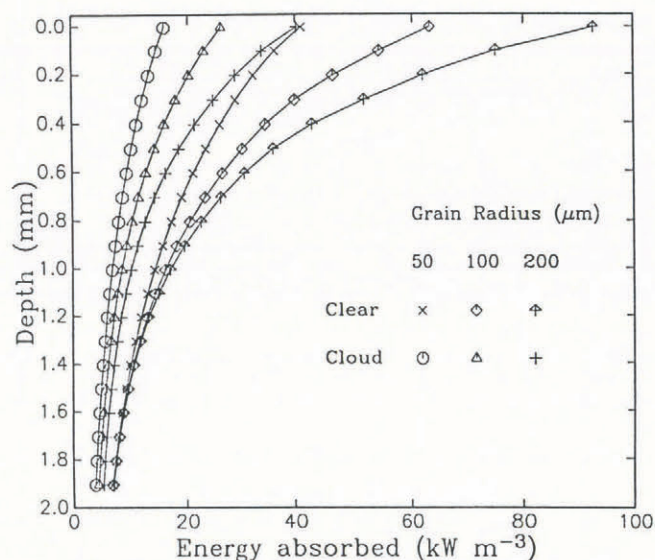


Fig. 5. Solar energy absorbed per unit volume, as a function of depth in the top 2 mm of the snow, for the spectral model with several grain-sizes and atmospheric conditions. This is the same quantity plotted in Figure 4 but on an expanded vertical scale.

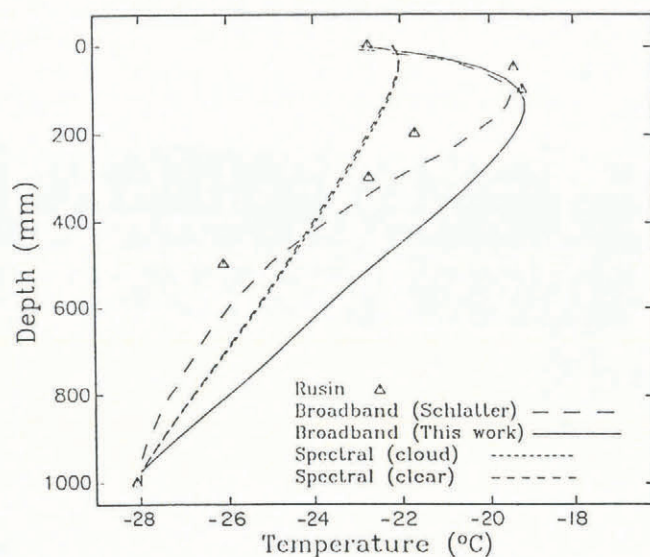


Fig. 6. Monthly average temperature as a function of depth in the top meter of the snow as reported by Rusin in December 1956 at Pioneerskaya (Antarctica) and as calculated by broad-band and spectral models. Incident solar flux is  $400 \text{ W m}^{-2}$ .

We now run Schlatter's coupled model of radiative transfer and heat conduction, to obtain steady-state temperature profiles in the snow. We compare the broad-band version of the model to the spectrally detailed version, using in both cases Schlatter's values for the boundary conditions, for snow density ( $380 \text{ kg m}^{-3}$ ) and for thermal conductivity ( $0.5 \text{ W m}^{-1} \text{ K}^{-1}$ ), which are reasonable for Antarctic snow.

The model snowpack was initially isothermal at  $-28^\circ\text{C}$ . After 10 d, the temperature profile reached a steady state, which is plotted in Figure 6 for both versions of the model together with Rusin's measurements and Schlatter's result. Our attempt to mimic Schlatter's model did not succeed completely. Our model does display a similar sub-surface maximum, but below that maximum we do not obtain the curvature in the temperature profile obtained by Schlatter. We can reproduce the curvature only, if steady state is not reached, by running the model less than 5 d. We also attempted to reproduce the curvature by invoking a time-dependent solar flux to model the diurnal variation in the solar zenith angle, but this did not significantly change the average temperature profile. However, the two broad-band models do emphatically agree on a temperature increase of nearly 4 K from the surface to 15 cm depth, in reasonable agreement with Rusin's measurement.

When we introduce spectral resolution, the sub-surface maximum shrinks to 0.2 K and moves toward the surface. For the spectral model, a grain-size of  $100 \mu\text{m}$  was used. While the average albedos were different for clear and cloudy sky (0.81 and 0.88), the temperature profiles were essentially the same, as the bulk of the heating occurred so near the surface that the snow was efficiently cooled by conduction. The effect of introducing the correct spectral dependence is thus to turn off the solid-state greenhouse in the case of dense snow on the Antarctic Plateau.

## FURTHER DISCUSSION OF TEMPERATURE MEASUREMENTS

The improvement in the model destroyed the agreement with Rusin's temperature measurements. This indicates that the model may have another error whose effect canceled the error due to coarse spectral resolution, or else that the measurements were in error. We have failed to find other flaws in Schlatter's model which would cause errors of similar magnitude to those caused by the broad-band approximation. However, there are reasons to doubt the validity of the measured temperature profile.

As noted above, Carroll (1982) failed to find sub-surface temperature maxima over the course of a summer at the South Pole. Ohmura (personal communication, 1988) did find a sub-surface temperature maximum in lake ice but never found it in snow, although he searched for it under a wide variety of conditions. He also concluded (Ohmura, 1984) that radiative heating must occur virtually at the surface to explain a lack of melting for the radiative conditions he observed. Ishikawa and Ishida (1970) performed laboratory experiments to search for conditions favoring sub-surface melting but they failed to produce any sub-surface temperature maximum in homogeneous snow. They adjusted their radiational heat input and wind velocities at the surface in an attempt to produce sub-surface melting. When the snow sample was covered with 1.5 cm of ice and subjected to a wind at its top surface of  $4.3 \text{ m s}^{-1}$ , a sub-surface temperature maximum of 3 K did result and caused melting at a depth of 4 cm. We are not certain of the explanation for this result but the situation may be similar to that of the blue ice discussed below.

We have attempted to match Rusin's measurement by varying the model's boundary conditions and snow conditions away from those reported by Rusin. Using the spectral model, we adjusted the latent- and sensible-heat flux at the surface over a wide range of values. While the surface temperature was sensitive to this change, the near-surface temperature gradient was not. We also tried allowing grain-size and density to vary with depth in the model over reasonable values measured in Antarctica ( $50\text{--}200 \mu\text{m}$  and  $300\text{--}400 \text{ kg m}^{-3}$ , respectively), and still could not develop Rusin's temperature profile. Finally, we attempted to enhance sub-surface heating by including in our model a uniform mixture of soot and snow using the method of Warren and Wiscombe (1980). The optimum amount of soot was found to be 1 ppm by mass but the sub-surface heating was enhanced by only 0.15 K. Soot contamination at this concentration is unlikely, since it would lower the snow albedo down to 0.74 from its measured value of 0.84. Furthermore, soot is present naturally in Antarctic snow only at about 0.2 ppb by mass; even near a large station, it reached only 3 ppb (Warren and Clarke, 1990). The fact that soot fails to boost the solid-state greenhouse effect significantly will be discussed in the context of the Matson and Brown model below. A thin layer of contaminated snow underlying a layer of clean snow could certainly induce a deeper volume heating but this would also lower the surface albedo, and is anyway an unlikely structure for Antarctic snow.

Radiative heating of thermistors could explain

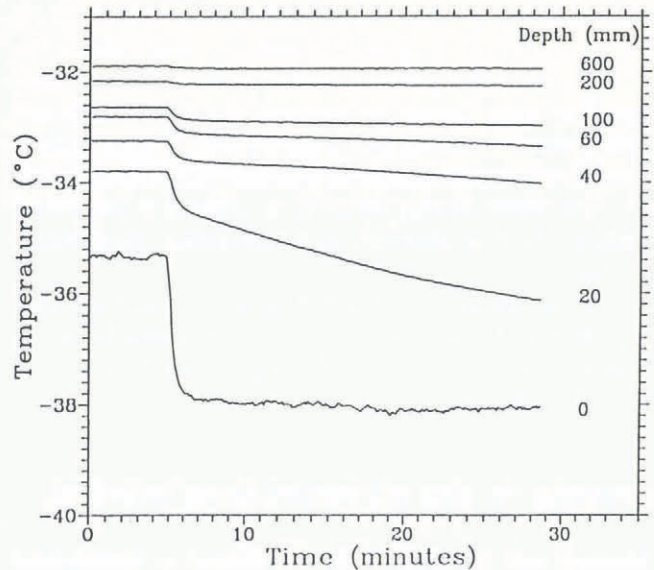


Fig. 7. Time series of sub-surface temperature, measured under clear sky near South Pole Station in January 1991. At time = 5 min, the site was shaded by a vertical sheet of plywood, blocking the direct solar beam but not the wind or the diffuse radiation from the sky. (The snow temperature increases with depth here but it is a transient effect: the surface-air temperature had dropped by 5 deg during the previous 3 d, causing the upper snow layers to cool.)

increased sub-surface temperatures, as it is difficult to design a temperature probe that matches the spectral absorption of snow. The thermistors would then have been at elevated temperatures, not measuring the snow temperature. Alley and others (1990) have emphasized the importance of shading the thermistors. We buried a string of calibrated thermistors, painted white to minimize radiative heating, near South Pole Station. After waiting 2 weeks for the temperatures to stabilize, the temperature profile was measured first with the site unshaded for 5 min, then shaded with a large sheet of plywood supported vertically. This shade blocked the direct solar beam but did not block wind or diffuse radiation from the sky. Figure 7 shows the time series of these temperatures. Initially, the thermistors cooled rapidly for about 1 min (as expected from the thermistors' small time constant), indicating that they had been reading a temperature higher than that of the snow they were in contact with. This was followed by a much slower cooling associated with the cooling of the snow, seen in all but the surface thermistor. As depth increased, cooling of both the thermistor and the snow decreased. Radiational heating of thermistors can be further minimized by covering them with aluminized mylar (personal communication from C. Stearns, 1992). Our current South Pole experiment shows this method is very effective, with a radiationally induced-temperature increase less than  $0.3^\circ\text{C}$  at the surface. These simple experiments suggest that it is difficult to measure temperature profiles of snow under direct sunlight, even with small, highly reflective thermistors. This effect may have contributed to the elevated temperatures at 10 cm depth reported by Rusin.

However, one might then expect Rusin's surface temperature to be the highest, unless it was measured

by a different method. Rusin did not give details of the experiment. If the reported "surface" temperature was the surface air temperature measured in a screen, it would not have been artificially elevated by solar absorption. (This was the case in the measurements of Niederdorfer (1933), whose sub-surface temperature rise of about 1 deg at 1 cm depth during January in Austria is sometimes cited as the first discovery of a sub-surface temperature maximum.)

In summary, we believe that the summertime temperature profile reported for Pioneerskaya by Rusin is in error but we cannot fully explain the causes of the experimental error.

## MODELS OF THE ICY SURFACE OF EUROPA

Matson and Brown (1989) developed a broad-band model to investigate the near-surface temperature profiles of icy satellites in the outer solar system. In the case of Europa, their model obtained sub-surface temperature increases as high as  $\approx 300$  K for "dirty" snow (all-wave albedo = 0.6) of low density ( $150 \text{ kg m}^{-3}$ ). However, this enormous greenhouse effect was partly due to the small value of heat conductivity they assumed ( $0.001 \text{ W m}^{-1} \text{ K}^{-1}$ ), which was later judged to be a factor of 10 too small. Fanale and Salvail collaborated with Matson and Brown (Fanale and others, 1990 (FSMB)) to perform the revised calculations with a more realistic heat conductivity of  $0.01 \text{ W m}^{-1} \text{ K}^{-1}$ , which is, however, still a factor of 50 smaller than that of Antarctic snow. We now examine the effect of introducing spectral resolution into the model for Europa. We first reproduce the results of FSMB with our broad-band two-stream model, then repeat the calculation with our spectral model.

The radiative-heating component of the FSMB model is essentially the same as in the Schlatter model, although there are differences in other aspects of the models, such as a modified bottom-boundary condition. Schlatter used a measured temperature at 1 m depth as a bottom-boundary condition. This allowed heat to be conducted out of the modeled region down to colder snow below. FSMB assumed for the case of Europa that below 2 m depth the satellite is isothermal at an unknown temperature. Their model therefore uses an insulating bottom-boundary condition, which allows no heat flow through the 2 m level. This bottom-boundary condition is useful for examining the solid-state greenhouse effect, as it uncouples the surface-energy fluxes from heating or cooling from below.

Using the parameters for Europa (table 2 of Matson and Brown (1989)), but with the larger heat conductivity used by FSMB, our broad-band model (Fig. 8) produces an average temperature profile which agrees with those in case 5 of FSMB. In order to apply our spectral model to the the case of Europa, we matched the low surface albedo of 0.6 by mixing 10 ppm carbon soot into the model snowpack of grain-size  $100 \mu\text{m}$ . (The magnitude of the solid-state greenhouse can be altered by varying the snow grain-size but FSMB constrained this parameter to a few hundred  $\mu\text{m}$  in diameter.) We calculated the optical properties of this dirty snow by the method of Warren and

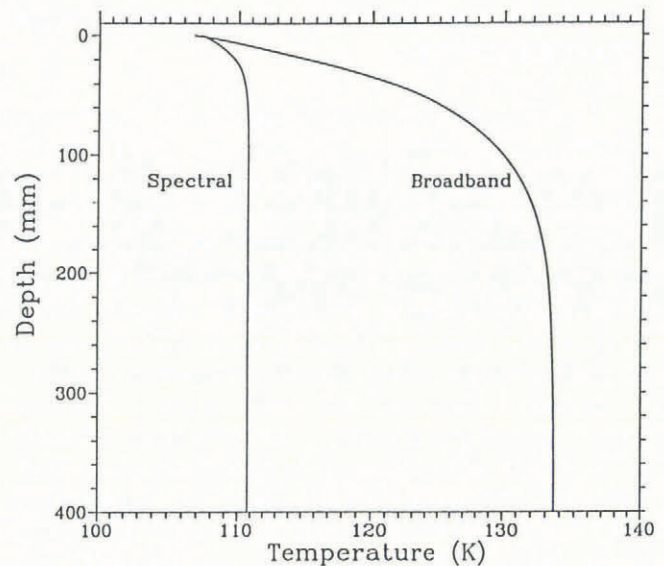


Fig. 8. Average temperature as a function of depth in the top meter of the snow surface of Jupiter's satellite Europa, as calculated by our broad-band and spectral models. Input values (Table 1) are those used by Matson and Brown (1989), except as modified by Fanale and others (1990). In particular, the thermal conductivity used by Fanale and others, and in this figure, is  $0.01 \text{ W m}^{-1} \text{ K}^{-1}$ , a factor of 10 lower than that used by Matson and Brown, leading to a factor of 7 reduction in the solid-state greenhouse effect in the broad-band model, and a factor of 9 reduction in the spectral model. The incident solar flux is  $17.4 \text{ W m}^{-2}$ .

Wiscombe (1980). When we introduced spectral resolution into the Europa model, the solid-state greenhouse shrank from 27 K to 4 K. The residual solid-state greenhouse of 4 K is due to the low conductivity of European snow (in comparison to Antarctic snow).

The FSMB model computed a diurnal cycle and also incorporated some other improvements which we have not included, in particular a more accurate numerical scheme, which caused their diurnal average surface temperature to be a few degrees higher than we obtain in Figure 8. However, our broad-band model agrees with theirs for the difference between surface and sub-surface temperatures, so we think the computed solid-state greenhouse effect on Europa would shrink by a factor of 6–7 if spectral resolution were introduced into the FSMB model.

It is interesting to note that the presence of impurities does not enhance the solid-state greenhouse. As Clow (1987, fig. 8) pointed out in a (spectrally resolved) model of Martian snowmelt, adding dust to the snow caused more absorption of solar radiation, but also caused it to be absorbed closer to the surface. The solid-state greenhouse effect is larger if the radiation is absorbed at greater depth, because it depends on the thermal-insulating property of the upper snow.

## THE SOLID-STATE GREENHOUSE EFFECT IN CLEAN SNOW

While we have shown that the solid-state greenhouse

effect is probably inconsequential in the uniform, clean, dense snow on the Antarctic Plateau, and probably small on the dirty surface of Europa, there remains the question of what conditions might favor significant sub-surface heating in snow or ice. The solid-state greenhouse is sensitive to thermal conductivity and hence to the density of the snowpack. Grain-size is also important, as it influences solar-radiation penetration. To investigate these dependences, we consider a hypothetical case using the surface and atmospheric conditions on the Antarctic Plateau, with an insulating bottom-boundary condition to maximize the solid-state greenhouse. Otherwise, we use the same conditions as in the spectral model in Figure 6, except that density and hence conduction are varied.

We use an empirical function for the dependence of thermal conductivity  $\kappa$  on density  $\rho$ , by fitting the compilation of Anderson (1976, fig. 3.1):

$$\kappa = 0.021 + 2.5\rho^2 \tag{8}$$

where  $\kappa$  is in  $\text{W m}^{-1} \text{K}^{-1}$  and  $\rho$  is in  $\text{Mg m}^{-3}$ . This formula gives the correct values for pure ice ( $\kappa = 2.1 \text{ W m}^{-1} \text{K}^{-1}$ ) and for pure air, and is meant to include the sum of all modes of heat transfer in snow: conduction, convection, latent-heat transfer and radiation across the void spaces, because these were not separated in the experiments reviewed by Anderson. (Using much of the same experimental data, Yen (1981) obtained an alternative empirical fit,

$$\kappa = 2.2362\rho^{1.885}.$$

Although Yen's formula does not give the correct limiting values for air and ice, it does agree well with Equation (8) for typical values of snow density. These formulas are both meant to apply at temperatures not far below the melting point. As temperature decreases, the conductivity of pure ice increases (fig. 14 of Yen (1981)), but the vapor density decreases; the combined effect is a decrease in effective conductivity by about a factor of 2 as the temperature drops from  $-5^\circ$  to  $-88^\circ\text{C}$  (fig. 16 of Yen (1981).)

The temperature profiles in Figure 9 show that the solid-state greenhouse can be quite large at low snow densities, suggesting that it may be important in promoting the metamorphism of low-density snow as in certain cases described by Colbeck (1989). However, Colbeck obtained an average daily sub-surface temperature maximum at 13 cm depth for a snow density of  $300 \text{ kg m}^{-3}$  (his fig. 5). Colbeck (personal communication, 1992) attributed this deep sub-surface heating to his choice of a low conductivity, but we believe that it is also because of his use of the broad-band approximation. Nevertheless, recent accurate measurements have found the temperature to reach its maximum within the topmost centimeter. In central Greenland, in summer, Alley and others (1990) observed a temperature rise of several degrees 5–10 mm below the surface during most of the day, causing loss of mass by sublimation and reducing the snow density from  $380$  to  $220 \text{ kg m}^{-3}$ . Because the less-dense snow has lower conductivity, there is a positive feed-back in this process.

We examined this situation using the spectral model with 2 mm vertical resolution, imposing an incident solar

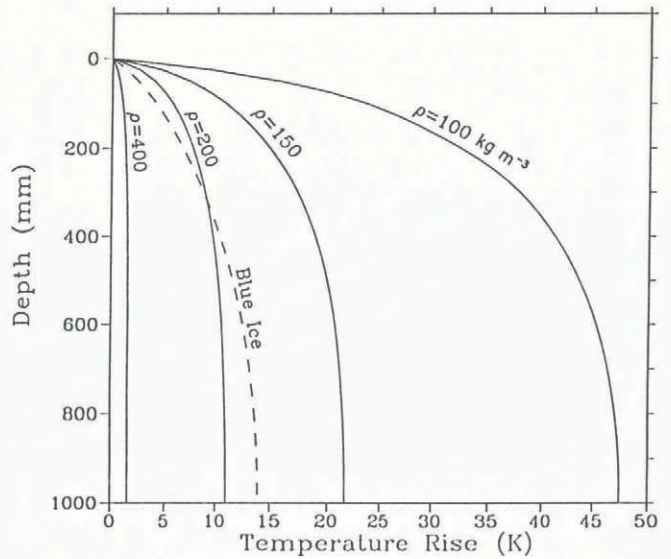


Fig. 9. Average temperature as a function of depth in the top meter of the snow surface, computed with the spectral model, with the same input values used in Figure 6, but for the hypothetical case of an insulating lower boundary. The blue ice has no internal scattering, an albedo of 0.07 (due to Fresnel reflection at the surface) and thermal conductivity  $2.1 \text{ W m}^{-1} \text{K}^{-1}$ . The curve for  $\rho = 400 \text{ kg m}^{-3}$  is appropriate for Antarctic surface snow. The incident solar flux is  $400 \text{ W m}^{-2}$ . The insulating lower boundary exaggerates the solid-state greenhouse effect, so actual sub-surface temperature increases would be less than shown here. (Compare the curve for  $\rho = 400 \text{ kg m}^{-3}$  with Figure 6.)

flux of  $800 \text{ W m}^{-2}$  (for mid-day in June at  $72.6^\circ\text{N}$ ), specifying a lower boundary temperature of  $-15^\circ\text{C}$  at 25 cm (the bottom of the observed diurnal temperature wave) and a uniform snow density of  $220 \text{ kg m}^{-3}$ . After 4 h of mid-day illumination, a solid-state greenhouse of 3 K developed, with peak at 22 mm depth. The peak in the model temperature would have been closer to the surface, in better agreement with the observations, if we had included the vertical variation of density, with denser (more conductive) snow ( $\rho = 380 \text{ kg m}^{-3}$ ) underlying the upper mass-loss layer. This sub-surface temperature maximum is much larger than that computed by the spectral model in Figure 6, for two reasons: (a) a mid-day solar flux is used here, rather than a diurnal average, and (b) the conductivity is reduced by a factor of 3.5 because of the low density.

As the snow density increases, so does the conduction of heat through the snow, while the penetration of sunlight into the snow decreases. These two effects make density the dominant variable controlling the solid-state greenhouse effect in snow. However, the snow grain-size is also important because it affects the penetration depth for solar radiation. Using the same parameters and boundary conditions used in Figure 9, the combined effects of density and grain-size are shown in Figure 10, where the temperature difference between the surface and 1 m depth is plotted versus density for three grain-sizes. Figures 9 and 10 use the insulating lower-boundary condition, and therefore exaggerate the solid-state greenhouse relative to

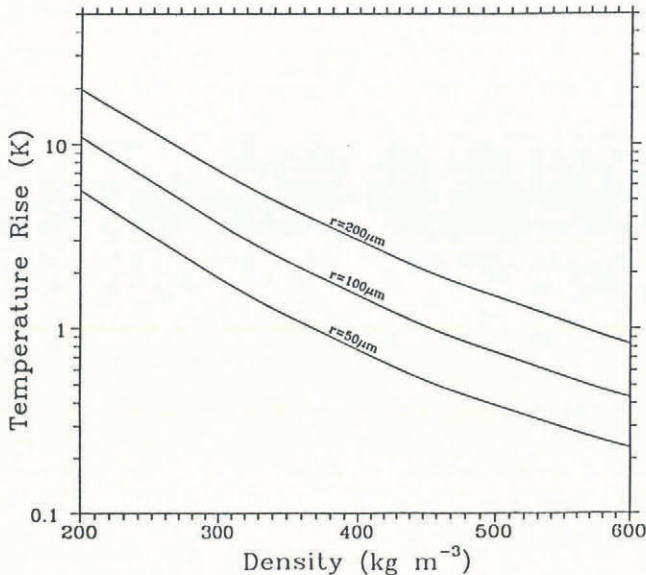


Fig. 10. Average solid-state greenhouse effect as a function of snow density for three values of snow-grain radius, computed with the spectral model. The same input values are used as in Figure 6, but for the hypothetical case of an insulating lower boundary, which exaggerates the greenhouse effect.

that shown in Figure 6. For example, the solid-state greenhouse in Figure 6 is 0.2 K but in Figure 9 it is 1.5 K for  $\rho = 400 \text{ kg m}^{-3}$ ; this difference is due solely to the difference in the lower-boundary condition. For low-density snow ( $\rho = 100 \text{ kg m}^{-3}$ ;  $\kappa = 0.05 \text{ W m}^{-2}$ ) the solid-state greenhouse is larger here than shown in Figure 8 for smaller  $\kappa$ . This is because the diurnal average incident solar flux is a factor of 23 larger at Pioneerskaya in December than on the equator of Europa.

### SUB-SURFACE HEATING IN BLUE ICE

Based on the arguments given above, we are skeptical that significant sub-surface heating occurs in dense Antarctic snow. However, sub-surface melting has been seen at the Antarctic coast in both shelf ice and fast sea ice, in places where strong winds remove the snow cover and expose patches of bare ice. The penetration of solar radiation into this bare ice has previously been discussed by Budd (1967).

Endo (1970) reported that on fast ice (15 m thick) near Syowa Station on the coast of East Antarctica "The surface of the uncovered ice was flat and clear with white patches of bubbly ice inlaid here and there. Puddles formed and developed in large numbers on the flat and clear parts, but few puddles were found in the white patches and on the general ice field covered with snow." The under-ice puddles were at 10–20 cm depth.

A similar phenomenon has been observed on wind-blown blue-ice areas on the Ross Ice Shelf (120 m thick) near McMurdo Station. Paige (1968) described these sub-surface melt pools as scattered patches of 10–15 m diameter, between 7 and 40 cm below the ice surface, and up to 1 m deep. A particular area where this blue ice

occurs, called the "Pegasus Site", is being considered as a late-summer air strip for wheeled aircraft. Mellor and Swithinbank (1989) suggested covering the runway with snow to prevent sub-surface melting.

To explain the sub-surface melting in blue ice, we applied the spectral model to the case of bubble-free (no internal scattering) pure ice with a surface albedo (Fresnel reflectance) of 0.07, and the same boundary conditions used for the other curves in Figure 9. The sub-surface temperature rose to about 14 K above the surface temperature (Fig. 9). The factors which favor the solid-state greenhouse in ice, relative to snow of  $\rho = 400 \text{ kg m}^{-3}$ , are the smaller extinction coefficient and the lower albedo. The ice absorbs about five times as much solar radiation as does the snow. The insulating lower-boundary condition exaggerates the possible solid-state greenhouse, because internal temperatures in ice shelves would in reality be well below freezing. The greenhouse effect is also exaggerated in the model because some internal scattering from air bubbles or ice-grain boundaries would occur in the real situation. The model supports the observations that melting as deep as 40 cm in blue ice can occur. The reason that sub-surface melting is relatively rare in Antarctica is due to the fact that snow cover is usually present.

### DISCUSSION

The solid-state greenhouse has sometimes been invoked to explain processes of snow metamorphism involving sublimation and redeposition of water vapor. For processes occurring in the top few millimeters of the snowpack, especially for low-density snow, the solid-state greenhouse can be important. This may be the case for firnspiegel on melting snow (LaChapelle, 1969, fig. 59), and depth hoar in the uppermost centimeter of the Greenland ice sheet (Alley and others, 1990). The diurnal cycle is also important in causing the temperature gradients which drive metamorphism. The "deflation" of sastrugi requires transport of water vapor and redeposition as hoar crystals (Gow, 1965), which could result from temperature gradients across the sastrugi which reverse sign as different faces of the sastrugi are illuminated by a low sun over the course of the day at the South Pole, even though the zenith angle remains constant.

The solid-state greenhouse can have great significance if a dark surface underlies a thin snow cover. The sub-snow vegetation warms by solar absorption, causing melting or sublimation of the snow in contact with it, forming hollow pockets of warm air around the stems and leaves, even while the air temperature above the snow is well below freezing. This phenomenon has been studied in Labrador–Ungava (personal communication from H. Granberg, 1981), and in central Alaska (personal communication from M. Sturm, 1991). The growing season begins before the snow has gone.

### CONCLUSIONS

To simulate the energy budget accurately for near-surface snow, radiative-transfer models must include some

spectral detail because the penetration depth for photons in snow of grain radius  $100\ \mu\text{m}$  and density  $400\ \text{kg m}^{-3}$  varies across the solar spectrum from  $240\ \text{mm}$  at  $0.47\ \mu\text{m}$  to  $0.4\ \text{mm}$  at  $2\ \mu\text{m}$  wavelength. Broad-band models greatly overestimated the depth of absorbed solar radiation. By using "average" values for penetration depth and absorption coefficient, these models were unable to make the important distinction that the wavelengths which are absorbed are not those that penetrate. It is not necessary to subdivide the solar spectrum into 118 bands as we have done; ten would probably be adequate for computing temperature profiles.

The solid-state greenhouse effect was found to be small when the spectral model was applied to clean snow on the Antarctic Plateau. In order to produce a significant near-surface temperature maximum with this effect, radiative heating must occur deep enough so that conductive heat transfer to the surface will be inefficient in removing heat, allowing a temperature gradient to be sustained. However, with the spectral model, most of the radiative heating occurs in the top 2 mm, and conduction is efficient in removing this energy up to the surface. The addition of an absorptive impurity to snow in the model only marginally enhanced the solid-state greenhouse because the penetration depth of solar radiation decreased, compensating for the increase in absorbed radiation. Although the solid-state greenhouse is insignificant for pure dense snow, it could be important for other media where the absorption coefficient varies with wavelength much less than shown in Figure 2a, and it is also important for low-albedo ice, where little scattering takes place; and for low-density snow, where the thermal conductivity is small.

## ACKNOWLEDGEMENTS

We thank A. Ohmura for stimulating us to undertake this project. We also benefited from discussions with C. Bohren, R. Brown, W. Budd, J. Carroll, G. Clow, S. Colbeck, K. Cuffey, T. Grenfell, M. Kuhn, D. Matson, A. Nolin, C. Raymond and T. Schlatter. The article by Ishikawa and Ishida (1970) was translated from Japanese into English by P. Corne and is available from S. G. W. Some of the computations were done at the U.S. National Center for Atmospheric Research. The research was supported by U.S. National Science Foundation grants ATM-86-05134 and DPP-88-18570.

## REFERENCES

- Alley, R. B., E. S. Saltzman, K. M. Cuffey and J. J. Fitzpatrick. 1990. Summertime formation of depth hoar in central Greenland. *Geophys. Res. Lett.*, **17**(12), 2393–2396.
- Anderson, E. A. 1976. A point energy and mass balance model of a snow cover. *NOAA Tech. Rep.* NWS-19.
- Bohren, C. F. 1987. Multiple scattering of light and some of its observable consequences. *Am. J. Phys.*, **55**(6), 524–533.
- Brown, R. H. and D. L. Matson. 1987. Thermal effects of insolation propagation into the regoliths of airless bodies. *Icarus*, **72**, 84–94.
- Budd, W. 1967. Ablation from an Antarctic ice surface. In Ōura, H., ed. *Physics of snow and ice*. Sapporo, Hokkaido University. Institute of Low Temperature Science, 431–446.
- Carroll, J. J. 1982. Long-term means and short-term variability of the surface energy balance components at the South Pole. *J. Geophys. Res.*, **87**(C6), 4277–4286.
- Choudhury, B. 1981. Radiative properties of snow for clear sky solar radiation. *Cold Reg. Sci. Technol.*, **4**(2), 103–120.
- Clow, G. D. 1987. Generation of liquid water on Mars through the melting of a dusty snowpack. *Icarus*, **72**(1), 95–127.
- Colbeck, S. C. 1989. Snow-crystal growth with varying surface temperatures and radiation penetration. *J. Glaciol.*, **35**(119), 23–29.
- Coulson, K. L. 1975. *Solar and terrestrial radiation*. New York, Academic Press.
- Endo, Y. 1970. Puddles observed on sea ice from the time of their appearance to that of their disappearance in Antarctica. *Low Temp. Sci., Ser. A*, **28**, 203–213. [In Japanese with English abstract.]
- Fanale, F. P., J. R. Salvail, D. L. Matson and R. H. Brown. 1990. The effect of volume phase changes, mass transport, sunlight penetration, and densification on the thermal regime of icy regoliths. *Icarus*, **88**(1), 193–204.
- Gow, A. J. 1965. On the accumulation and seasonal stratification of snow at the South Pole. *J. Glaciol.*, **5**(40), 467–477.
- Grenfell, T. C. and G. A. Maykut. 1977. The optical properties of ice and snow in the Arctic Basin. *J. Glaciol.*, **18**(80), 445–463.
- Grenfell, T. C. and D. K. Perovich. 1981. Radiation absorption coefficients of polycrystalline ice from 400–1400 nm. *J. Geophys. Res.*, **86**(C8), 7447–7450.
- Ishikawa, N. and T. Ishida. 1970. An experimental study of local temperature increase in snow and ice. I. *Low Temp. Sci., Ser. A*, **28**, 165–173.
- Kuhn, M., L. S. Kundla and L. A. Stroschein. 1977. The radiation budget at Plateau Station, Antarctica, 1966–1967. *Antarct. Res. Ser.*, **25**, 45–73.
- Labs, D. and H. Neckel. 1970. Transformation of the absolute solar radiation data into the International Practical Temperature Scale of 1968. *Sol. Phys.*, **15**(1), 79–87.
- LaChapelle, E. R. 1969. *Field guide to snow crystals*. Seattle, WA, University of Washington Press.
- Liljequist, G. H. 1956. Energy exchange of an Antarctic snow-field: short-wave radiation (Maudheim  $71^{\circ}03' \text{S}$ ,  $10^{\circ}65' \text{W}$ ). *Norwegian-British-Swedish Antarctic Expedition, 1949–52. Sci. Results*, **2**(1A).
- Matson, D. L. and R. H. Brown. 1989. Solid-state greenhouses and their implications for icy satellites. *Icarus*, **77**(1), 67–81.
- Mellor, M. 1977. Engineering properties of snow. *J. Glaciol.*, **19**(81), 15–66.
- Mellor, M. and C. Swithinbank. 1989. Airfields on Antarctic glacier ice. *CRREL Rep.* 89-21.
- Neckel, H. and D. Labs. 1984. The solar radiation

- between 3300 and 12,500 Angstroms. *Solar Phys.*, **90**(2), 205–258.
- Niederdorfer, E. 1933. Messungen des Wärmeumsatzes über schneebedecktem Boden. *Meteorologische Zeitschrift*, **50**(6), 201–208.
- Ohmura, A. 1984. Comparative energy balance study for Arctic tundra, sea surface, glaciers and boreal forests. *GeoJournal*, **8**(3), 221–228.
- Paige, R.A. 1968. Sub-surface melt pools in the McMurdo Ice Shelf, Antarctica. *J. Glaciol.*, **7**(51), 511–516.
- Rusin, N.P. 1961. *Meteorological and radiational regime of Antarctica*. Jerusalem, Israel Program for Scientific Translations.
- Schlatter, T.W. 1972. The local surface energy balance and subsurface temperature regime in Antarctica. *J. Appl. Meteorol.*, **11**(10), 1048–1062.
- Schwerdtfeger, P. and G. Weller. 1977. Radiative heat transfer processes in snow and ice. *Antarct. Res. Ser.*, **25**, 35–39.
- Schwerdtfeger, W. 1970. The climate of the Antarctic. In Orvig, S., ed. *World survey of climatology. Vol. 14*. New York, Elsevier, 253–355.
- Warren, S.G. 1982. Optical properties of snow. *Rev. Geophys. Space Phys.*, **20**(1), 67–89.
- Warren, S.G. 1984. Optical constants of ice from the ultraviolet to the microwave. *Appl. Opt.*, **23**(8), 1206–1225.
- Warren, S.G. and A.D. Clarke. 1990. Soot in the atmosphere and snow surface of Antarctica. *J. Geophys. Res.*, **95**(D2), 1811–1816.
- Warren, S.G. and W.J. Wiscombe. 1980. A model for the spectral albedo of snow. II. Snow containing atmospheric aerosols. *J. Atmos. Sci.*, **37**(12), 2734–2745.
- Wiscombe, W.J. 1980. Improved Mie scattering algorithms. *Appl. Opt.*, **19**(9), 1505–1509.
- Wiscombe, W.J. and S.G. Warren. 1980a. A model for the spectral albedo of snow. I. Pure snow. *J. Atmos. Sci.*, **37**(12), 2712–2733.
- Wiscombe, W.J. and S.G. Warren. 1980b. Solar and infrared radiation calculations for the Antarctic Plateau using a spectrally-detailed snow reflectance model. *International Radiation Symposium Volume of Extended Abstracts*. Fort Collins, CO, Colorado State University.
- Wiscombe, W.J., R.M. Welch and W.D. Hall. 1984. The effects of very large drops on cloud absorption. Part I. Parcel models. *J. Atmos. Sci.*, **41**(8), 1336–1355.
- Yen, Y.C. 1981. Review of thermal properties of snow, ice, and sea ice. *CRREL Rep.* 81-10.

*The accuracy of references in the text and in this list is the responsibility of the authors, to whom queries should be addressed.*

*MS received 19 December 1989 and in revised form 6 January 1992*